Supplementary Document: Effect of nearby Metals on Electro-Quasistatic Human Body Communication

Samyadip Sarkar, Arunashish Datta, David Yang, Mayukh Nath
Student Member, IEEE, Shovan Maity, *Member, IEEE* and Shreyas Sen, *Senior Member, IEEE*

I. Transfer Function Derivation for Proximity-based Interaction with Ground-connected Metallic Object

The simplified circuit model for the proximity-based interaction between EQS HBC user and a ground-connected metallic object is presented in Supplementary Fig. 1. For the return path capacitances at the Tx and Rx, we define the return path capacitances in the absence of any surrounding conductive objects such as C_{xTx} and C_{xRx}. These values depend on the location of the devices (x) on the subject's body and the geometry of the devices, represented as C_{self}. Specifically, the return path capacitances are expressed in Eqs. 1, 1a.

$$C_{xTx} = xC_{selfTx} \tag{1}$$

$$C_{xRx} = xC_{selfRx} \tag{1a}$$

To distinguish between scenarios where ground-connected metallic objects are present and those where they are absent, we denote the net return path capacitance as C_{retTx} and C_{retRx}. These are mathematically expressed in Eqs. 2, 2a.

$$C_{retTx} = C_{xTx} + C_{GMTx} \tag{2}$$

$$C_{retRx} = C_{xRx} + C_{GMRx} \tag{2a}$$

Here, C_{GMTx} and C_{GMRx} represent the capacitances associated with the ground of the transmitter to the metallic object and from the ground of the receiver to the metallic object, respectively. Assuming C_B as the capacitance between the subject's body and Earth's ground when no other conductive objects are present in the surroundings. It is important to note that the presence of ground-connected metallic objects influences the subject's body capacitance. To differentiate between scenarios in which ground-connected metallic objects are present and those in which they are absent, we denote the net body capacitance (including ground-connected metals) as C_{Body}. This is expressed mathematically in Eq. 3.

$$C_{Body} = C_B + C_{BM} \tag{3}$$

where C_{BM} represents the capacitance between the subject's body and the metallic object. Assuming the effect of inter-device coupling capacitance ($C_C < 1$ fF) to be negligible for Tx and Rx at more than 50 cm apart. The return path impedance being orders of magnitude higher than the impedance contribution of Z_{Body} i.e., $Z_{Body} << Z_{ret}$, the induced potential on subject's body (V_B) is formulated in Eq. 4.

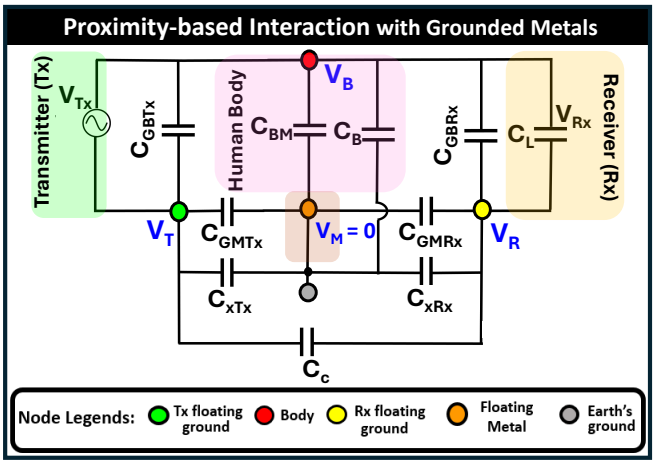

Fig. 1: Simplified equivalent circuit model for proximity-based interaction between subject and ground-connected metals.

$$V_B = \frac{Z_{Body}}{Z_{Body} + Z_{retTx}} V_{Tx} \approx \frac{Z_{Body}}{Z_{retTx}} = \left(\frac{C_{retTx}}{C_B}\right) V_{Tx} \tag{4}$$

Now, a fraction of V_B gets picked-up at the receiver and the received voltage (V_{Rx}) as a function of V_B is presented in Eq. 5.

$$V_{Rx} = \frac{Z_{L(eff.)}}{Z_{L(eff.)} + Z_{retRx}} V_{Tx} \approx \frac{Z_{L(eff.)}}{Z_{retRx}} = \left(\frac{C_{retRx}}{C_{L(eff.)}}\right) V_B \tag{5}$$

"This work was supported by Quasistatics, Inc. under Grant 40003567
Samyadip Sarkar, Arunashish Datta, David Yang, Mayukh Nath, Shreyas Sen are with Elmore Family School of Electrical and Computer Engineering, Purdue University, West Lafayette, IN, USA (e-mail: {sarkar46, datta30, yang996, shreyas}@purdue.edu, nathm@alumni.purdue.edu).
Shovan Maity is with Quasistatics Inc. USA (e-mail: shovan@10xar.com).

Hence, the transfer function is formulated by combining Eq. 4 and Eq. 5 and is presented in Eq. 6.

$$T_{NTGM}(s) = \frac{V_{Rx}}{V_{Tx}}(s) \approx \frac{Z_{Body}}{Z_{retTx}} \times \frac{Z_{L(eff.)}}{Z_{retRx}} \approx \frac{C_{retTx}}{C_{Body}} \times \frac{C_{retRx}}{C_{L(eff.)}} \tag{6}$$

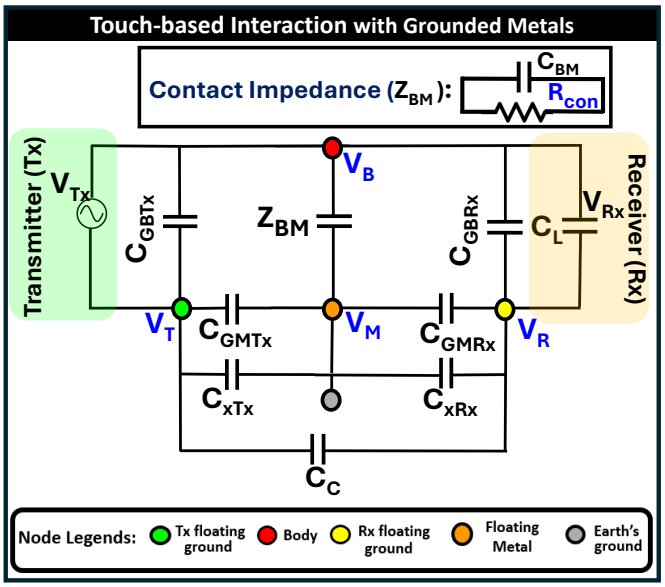

Fig. 2: Simplified equivalent circuit model for touch-based interaction between subject and ground-connected metallic obejcts.

II. Transfer Function Derivation for Touch-based Interaction with Ground-Connected Metallic Object

For the touch-based interaction with ground-connected metallic object, the impedance (Z_{BM}) between the body and the grounded metallic object considered to be the parallel combination of the contact resistance (R_{con}) and the contact capacitance (C_{BM}), shown in the equivalent circuit model in Supplementary Fig. 2. Hence, the expression for Z_{BM} is formulated in Eq. 7.

$$Z_{BM}(s) = \frac{R_{con}}{1 + sR_{con}C_{BM}} \tag{7}$$

Now, in the impedance based transfer function derived in Eq. 6, substituting the value of Z_{BM}, we get the transfer function for touch-based interactions (T_{TGM}), derived in Eq. 8.

$$T_{TGM}(s) = \frac{V_{Rx}}{V_{Tx}}(s) \approx \frac{\frac{R_{con}}{1+sR_{con}C_{BM}}}{\frac{1}{sC_{retTx}}} \times \frac{\frac{1}{sC_{L(eff.)}}}{\frac{1}{sC_{retRx}}} \approx \left(\frac{C_{retTx}C_{retRx}}{C_{L(eff.)}C_{BM} + \left(\frac{C_{L(eff.)}}{sR_{con}}\right)} \right) \tag{8}$$

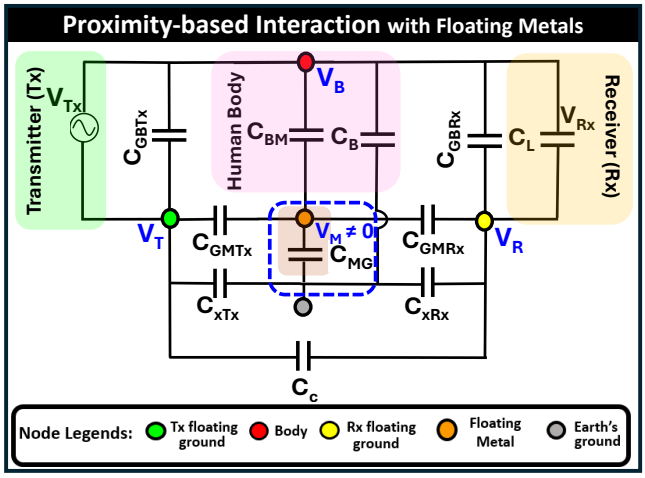

Fig. 3: Simplified equivalent circuit model for touch-based interaction between subject and Floating metallic obejcts.

III. Transfer Function Derivation Proximity & Touch-based Interaction with Floating Ground Metallic Object

The circuit model illustrating the proximity-based interaction between a user of EQS HBC and a floating metallic object is shown in Supplementary Fig. 3. Assuming the voltages at the following nodes: ground of the Tx, ground of the Rx, subject's body, and metal object are at potential V_T, V_R, V_B, and V_M respectively. Applying Kirchhoff's Current Law (KCL) at the node with potential V_T, equation relating these above four nodal voltages is expressed in Eq. 9.

$$(C_B + C_{BM})V_B + (C_{xTx} + C_{GMTx})V_T - C_{L(eff.)}V_R - (C_{GMTx} + C_{BM})V_M = 0 \tag{9}$$

Similarly, by KCL at the earth's ground node, we get the relation expressed in Eq. 10.

$$C_B V_B + C_{xTx}V_T + C_{xRx}V_R + = 0 \tag{10}$$

Then, by KCL at the node with potential V_M, we get the relation expression in Eq. 11.

$$C_{BM}V_B + C_{GMTx}V_T + C_{GMRx}V_R - (C_{MG} + C_{GMRx} + C_{GMTx} + C_{BM})V_M = 0 \tag{11}$$

Hence, the induced potential on the metallic object (V_M) is presented in Eq. 12.

$$V_M = \frac{C_{BM}}{C_A}V_B + \frac{C_{GMRx}}{C_A}V_R + \frac{C_{GMTx}}{C_A}V_T \tag{12}$$

where,

$$C_A = (C_{MG} + C_{GMRx} + C_{GMTx} + C_{BM}) \tag{12a}$$

For a large object, the expression for C_A can be approximately simplified as $C_A \approx (C_{MG} + C_{BM})$ (Since, C_{GMRx}, C_{GMTx} $<< C_{MG}$, C_{BM}). The coupling between the body-to-metallic object (C_{BM}) changes with the change in the average distance and orientation of subject relative to the metallic object. Now,

by KCL at the node with potential V_R, we get the relation expression in Eq. 13.

$$C_{L(eff.)}V_B-(C_{L(eff.)}+C_{xRx}+C_{GMRx})V_R-C_{GMRx}V_M=0 \tag{13}$$

Since, the subject's body potential (V_B) also changes under the influence of metallic objects in the surroundings. Incorporating the effect from the surrounding metals, the nodal voltage at the ground of the Rx is expressed in Eq. 14.

$$V_R=\frac{B}{P}V_B+\frac{Q}{P}V_T \tag{14}$$

where P, Q, and B take the following form:

$$P=\frac{1}{C_{L(eff.)}}\left[(C_{L(eff.)}+C_{xRx}+C_{GMRx})-\frac{C_{GMRx}^2}{C_A}\right] \tag{14a}$$

$$Q=\frac{C_{GMRx}C_{GMTx}}{C_{L(eff.)}C_A} \tag{14b}$$

$$B=1+\frac{C_{GMRx}C_{BM}}{C_{L(eff.)}C_A} \tag{14c}$$

$$C_{L(eff.)}=C_{GBRx}+C_L \tag{14d}$$

A generalized circuit model for the interaction between

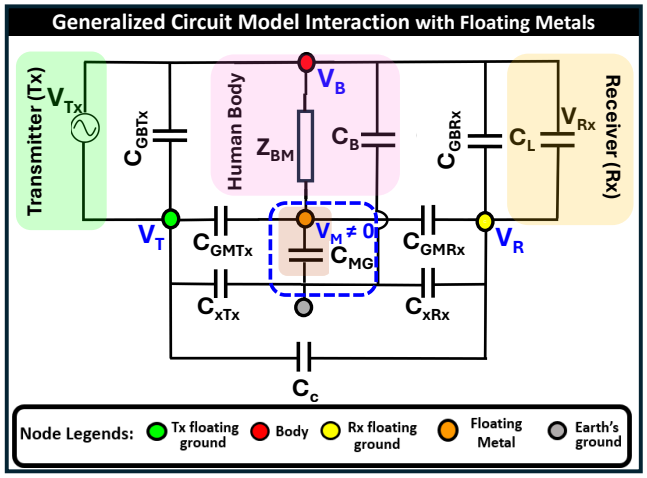

Fig. 4: Generalized circuit model for interaction between subject and Floating metallic obejcts.

EQS HBC user and a floating metallic object is presented in Supplementary Fig. 4. By KCL at node M, we obtain the expression for V_B in relation to V_M, V_T, and V_R, presented in Eq. 15.

$$\begin{aligned}V_B=&\left(1+s\left(C_{GMRx}+C_{GMTx}+C_{MG}\right)Z_{BM}\right)V_M\\&-sC_{GMRx}Z_{BM}V_R-sC_{GMTx}Z_{BM}V_T\end{aligned} \tag{15}$$

By KCL at the ground node of the Rx, we obtain another equation relating V_R with V_B and V_M, presented in Eq. 16.

$$V_R\left(C_{xRx}+C_{L(\text{eff.})}+C_{GMRx}\right)=C_{L(\text{eff.})}V_B+C_{GMRx}V_M \tag{16}$$

Again, by KCL at the ground node, we obtain another expression relating V_B, V_R and V_T, presented in Eq. 17.

$$C_BV_B+C_{xRx}V_R+C_{xTx}V_T=0 \tag{17}$$

where, V_T can be expressed as

$$V_T=-(\frac{C_B}{C_{xTx}}V_B+\frac{C_{xRx}}{C_{xTx}}V_R) \tag{17a}$$

By substituting V_T from Eq. 17a in the expression for V_B in Eq. 15, we obtain

$$V_B=\frac{D}{A}V_M+\frac{F}{A}V_R \tag{18}$$

where A, D and F are defined in Eq. 18 (a, b, c)

$$A=1-sC_{GMTx}Z_{BM}\frac{C_B}{C_{xTx}} \tag{18a}$$

$$D=1+s(C_{GMRx}+C_{GMTx}+C_{MG})Z_{BM} \tag{18b}$$

$$F=(sC_{GMTx}\frac{C_{xRx}}{C_{xTx}}-sC_{GMRx})Z_{BM} \tag{18c}$$

Now, V_{Tx} can be written in relation to V_B and V_T, expressed in Eq. 19.

$$V_{Tx}=V_B-V_T \tag{19}$$

Substituting V_T and rearranging terms, we get

$$V_{Tx}=UV_B+TV_R \tag{19a}$$

where U and T are defined in Eq. 19 (b, c)

$$U=1+\frac{C_B}{C_{xTx}} \tag{19b}$$

$$T=\frac{C_{xRx}}{C_{xTx}} \tag{19c}$$

Now, V_M can be expressed in terms of V_B and V_R, presented in Eq. 20 can be written as

$$V_M=SV_B+RV_R \tag{20}$$

where S and R are defined in Eq. 20 (a, b)

$$S=-\frac{C_{L(eff.)}}{C_{GMRx}} \tag{20a}$$

$$R=\frac{C_{xRx}+C_{L(eff.)}+C_{GMRx}}{C_{GMRx}} \tag{20b}$$

Hence, the transfer function is formulated in Eq. 21

$$T_{NTFM}(s)=\frac{V_{Rx}}{V_{Tx}}=\frac{V_B-V_R}{V_B-V_T}\approx\left(\frac{1-\frac{(A-DS)}{DR+F}}{U+T\frac{(A-DS)}{DR+F}}\right) \tag{21}$$

Similar to grounded metal, during touch-based interaction with floating metal, the transfer characteristics ($T_{TFM}(s)$) can be obtained by substituting the expression of Z_{BM} from Eq. 7.

IV. Derivation of the Sensitivity Analysis

Since, the channel transfer function is defined as

$$\begin{aligned}T&=\frac{V_{\text{Rx}}}{V_{\text{Tx}}}=\frac{V_B}{V_{Tx}}\times\frac{V_{Rx}}{V_B}\\&=\frac{C_{\text{retTx}}}{C_{\text{retTx}}+C_{\text{Body}}}\times\frac{C_{\text{retRx}}}{C_{\text{retRx}}+C_{\text{L(eff.)}}}\end{aligned}$$

The relative sensitivity of T to a small change in C_i is expressed in Eq. 22

$$S_{C_i}=\frac{C_i}{T}\frac{\partial T}{\partial C_i} \tag{22}$$

A. Sensitivities of $\frac{V_B}{V_{Tx}}$

$$\frac{\partial\left(\frac{V_B}{V_{Tx}}\right)}{\partial C_{\mathrm{retTx}}} = \frac{C_{\mathrm{Body}}}{\left(C_{\mathrm{retTx}} + C_{\mathrm{Body}}\right)^2} \tag{23a}$$

$$\frac{\partial\left(\frac{V_B}{V_{Tx}}\right)}{\partial C_{\mathrm{Body}}} = -\frac{C_{\mathrm{retTx}}}{\left(C_{\mathrm{retTx}} + C_{\mathrm{Body}}\right)^2} \tag{23b}$$

Hence, the relative sensitivities are defined in Eq. 23c, 23d.

$$S_{C_{\mathrm{retTx}}} = \frac{C_{\mathrm{retTx}}}{\left(\frac{V_B}{V_{Tx}}\right)} \frac{\partial\left(\frac{V_B}{V_{Tx}}\right)}{\partial C_{\mathrm{retTx}}} = \frac{C_{\mathrm{Body}}}{C_{\mathrm{retTx}} + C_{\mathrm{Body}}} \tag{23c}$$

$$S_{C_{\mathrm{Body}}} = \frac{C_{\mathrm{Body}}}{\left(\frac{V_B}{V_{Tx}}\right)} \frac{\partial\left(\frac{V_B}{V_{Tx}}\right)}{\partial C_{\mathrm{Body}}} = -\frac{C_{\mathrm{Body}}}{C_{\mathrm{retTx}} + C_{\mathrm{Body}}} \tag{23d}$$

B. Sensitivities of $\frac{V_{Rx}}{V_B}$

$$\frac{\partial\left(\frac{V_{Rx}}{V_B}\right)}{\partial C_{\mathrm{retRx}}} = \frac{C_{\mathrm{L(eff.)}}}{\left(C_{\mathrm{retRx}} + C_{\mathrm{L(eff.)}}\right)^2} \tag{24a}$$

$$\frac{\partial\left(\frac{V_{Rx}}{V_B}\right)}{\partial C_{\mathrm{L(eff.)}}} = -\frac{C_{\mathrm{retRx}}}{\left(C_{\mathrm{retRx}} + C_{\mathrm{L(eff.)}}\right)^2} \tag{24b}$$

$$S_{C_{\mathrm{retRx}}} = \frac{C_{\mathrm{retRx}}}{\left(\frac{V_{Rx}}{V_B}\right)} \frac{\partial\left(\frac{V_{Rx}}{V_B}\right)}{\partial C_{\mathrm{retRx}}} = \frac{C_{\mathrm{L(eff.)}}}{C_{\mathrm{retRx}} + C_{\mathrm{L(eff.)}}} \tag{24c}$$

$$S_{C_{\mathrm{L(eff.)}}} = \frac{C_{\mathrm{L(eff.)}}}{\left(\frac{V_{Rx}}{V_B}\right)} \frac{\partial\left(\frac{V_{Rx}}{V_B}\right)}{\partial C_{\mathrm{L(eff.)}}} = -\frac{C_{\mathrm{L(eff.)}}}{C_{\mathrm{retRx}} + C_{\mathrm{L(eff.)}}} \tag{24d}$$

The combined sensitivity can be obtained by putting these sensitivities expressed in Eqs. 23c, 23d, 24c, 24d, together and is expressed in Eqs. 25 and 25a.

$$\frac{\partial T}{\partial C_i} = \left(\frac{V_{Rx}}{V_B}\right) \frac{\partial\left(\frac{V_B}{V_{Tx}}\right)}{\partial C_i}, \quad C_i \in \{C_{\mathrm{retTx}}, C_{\mathrm{Body}}\} \tag{25}$$

$$\frac{\partial T}{\partial C_j} = \left(\frac{V_B}{V_{Tx}}\right) \frac{\partial\left(\frac{V_{Rx}}{V_B}\right)}{\partial C_j}, \quad C_j \in \{C_{\mathrm{retRx}}, C_{\mathrm{L(eff.)}}\} \tag{25a}$$

V. Electric Field Variation inside Elevator

The variations in the coupled E-Field strength from the subject's body to the walls of the metallic enclosure for different positions of the subject inside an elevator are illustrated in Supplementary Fig. 5. Considerable reduction in the coupled E-field strength on the subject's body is observed when the human leans on the elevator face wall through the torso.

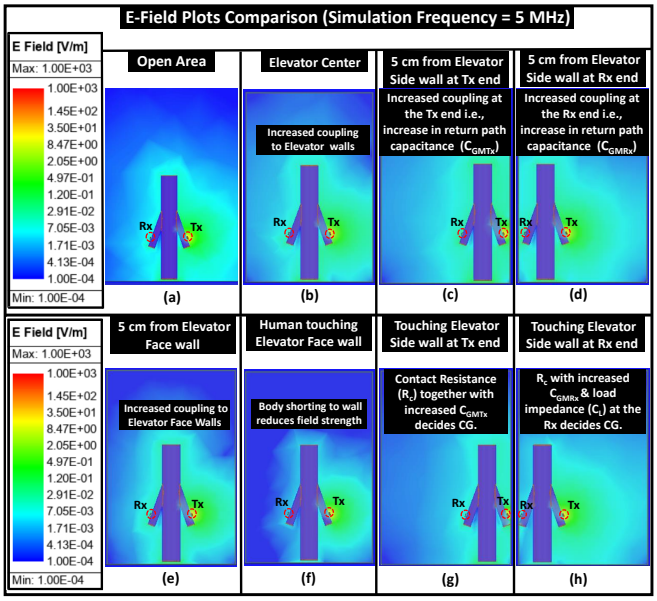

Fig. 5: Comparative analysis of the E-Field plots under different scenarios in metallic enclosure: The following scenarios are illustrated: (a) In an Open Area, (b) At the elevator center, (c) 5 cm from the wall at the Tx end, (d) 5 cm from the wall at the Rx end, (e) Subject's torso is at 5 cm from face wall, (f) Subject is leaning on the face wall, (g) Human touching side wall at the Tx side, (h) human touching side wall at the Rx side.

VI. Performance Analysis of the Communication Channel

The presence of metallic objects within the leakage limit (∼5 cm from the subject's body and ∼20 cm from communication devices, such as the transmitter (Tx) and receiver (Rx)) affects the parasitic return paths of Electro-quasistatic (EQS) Human Body Communication (HBC). This phenomenon is expected to impact the performance of wireless body-centric communication. In this analysis, we investigate the impact of nearby metallic objects on the performance of the body channel by examining variations in Signal-to-Noise Ratio (SNR), Shannon capacity, and bit error rate for different modulation schemes. These schemes include On-Off Keying (OOK), commonly referred to as Pulse Amplitude Modulation (PAM-2), Quadrature Amplitude Modulation (QAM), and Binary Phase Shift Keying (BPSK). We assume a white noise floor of 5 nV/$\sqrt{\mathrm{Hz}}$. Let the nominal return-path capacitances and body capacitances be $\mathrm{C_{xTx}}$, $\mathrm{C_{xRx}}$, and $\mathrm{C_B}$, and let the metal-induced perturbations be $\mathrm{C_{GMTx}}$, $\mathrm{C_{GMRx}}$, and $\mathrm{C_{Body}}$. Then the net capacitances become $\mathrm{C_{retTx}}$, $\mathrm{C_{retRx}}$, and $\mathrm{C_{Body}}$ The resulting EQS-HBC channel gain is presented in Eq. 26.

$$T = \frac{C_{\mathrm{retTx}}}{C_{\mathrm{retTx}} + C_{\mathrm{Body}}} \times \frac{C_{\mathrm{retRx}}}{C_{\mathrm{retRx}} + C_{\mathrm{L(eff.)}}} \tag{26}$$

Assume a transmit RMS voltage $\mathrm{V_{Tx}}$ and white noise power spectral density (PSD): $\mathrm{N_0} = \left(5 \times 10^{-9}\right)^2 = 25 \times 10^{-18}\mathrm{V^2/Hz}$. Over an operational channel bandwidth B, the noise variance is $\mathrm{N_0B}$. The received signal power (P_{sig}) is

presented in Eq. 27

$$P_{\text{sig}} = \left|TV_{\text{Tx}}\right|^2 \quad P_{\text{noise}} = N_0\, B \tag{27}$$

From the Eq. 26 and 27 the obtained SNR is presented in Eq. 28.

$$SNR = \frac{P_{\text{sig}}}{P_{\text{noise}}} = \frac{|T|^2\, V_{\text{Tx}}^2}{N_0\, B} \tag{28}$$

Hence, from the obtained SNR and bandwidth, the channel capacity is expressed in Eq. 29

$$\text{Channel Capacity (bits/s)} = B \log_2(1 + SNR) \tag{29}$$

Now, the BER expressions for various modulation schemes as a function of SNR are presented in Eqs. 30a, 30b, 30c.

$$\text{BER}_{\text{OOK}} = Q\big(\sqrt{\gamma}\big) \tag{30a}$$

$$\text{BER}_{\text{QPSK}} = Q\big(\sqrt{2\,\gamma}\big) \tag{30b}$$

$$\text{BER}_{M\text{-QAM}} = \frac{4(\sqrt{M}-1)}{\sqrt{M}\,\log_2 M}\, Q\Big(\sqrt{\frac{3\,\gamma\,\log_2 M}{M-1}}\Big) \tag{30c}$$

where Q is defined in Eq. 30d

$$Q(x) = \frac{1}{\sqrt{2\pi}} \int_x^{\infty} e^{-t^2/2}\, dt \tag{30d}$$

in the above expressions γ is related to SNR by how bit-energy over the noise band. In particular, transmitting at bit-rate of R_b over a noise bandwidth B, the signal power is defined as $\text{P}_\text{s}\text{ig} = \text{E}_\text{b}\,\text{R}_\text{b}$, hence the SNR is expressed in Eq. 31.

$$\frac{P_{sig}}{P_{noise}} = \frac{E_b\, R_b}{N_0\, B} = \frac{E_b}{N_0} \cdot \frac{R_b}{B} \tag{31a}$$

$$\gamma = \frac{E_b}{N_0} = SNR \times \frac{B}{R_b} \tag{31b}$$

Assuming the bit-rate to be the same as operational bandwidth ($R_b = B$), we get $\gamma = SNR$.

Now, with operational bandwidth (B) of 5 MHz, $\text{V}_{\text{Tx}} = 1\text{V}$, assuming a noise floor of -70 dBV for CMOS-based body-communication receiver, capacitances (C_{xTx}, C_B, C_{xRx}, $\text{C}_{\text{L(eff.)}}$) being (0.2, 150, 0.2, 5) pF in open area, if the surrounding metal induced perturbations being Δ (C_{xTx}, C_B, C_{xRx}, $\text{C}_{\text{L(eff.)}}$): (0.8, 0, 0.8, 0) pF, i.e., (C_{retTx}, C_{Body}, C_{retRx}, $\text{C}_{\text{L(eff.)}}$): (1, 150, 1, 5) pF, $T \approx 0.0013$, $SNR \approx 12.49$ dB. Over a bandwidth of 5 MHz, channel capacity comes around 21.1 Mbps. The the ideal-coherent BER for OOK comes 1×10^{-5} that satisfies the intended uncoded BER requirements for OOK (10^{-2}). The variation in performance metrics with the change in C_{retTx} and C_{Body} is captured in Supplementary Fig. 6. In summary, it can be interpreted as, an increase in C_{retTx} leads to an enhanced channel capacity (i.e., $\sim$10 Mbps increase in channel capacity with 100% increase in C_{retTx}) from the improved SNR, illustrated in Supplementary Fig. 6(a). The variation in ideal-coherent BER with C_{Body} for different modulation schemes like OOK, QPSK, and 16-QAM, presented in Supplementary Fig. 6(b), shows an increase in C_{Body} facilitates reliable communication at reduced BER. On contrary, a rise in C_{Body} reduces the channel capacity owing to an attenuation in SNR, represented in Supplementary Fig. 6(c). The BER also exhibit an increasing trend with increasing C_{Body}, shown in Supplementary Fig. 6 (d).

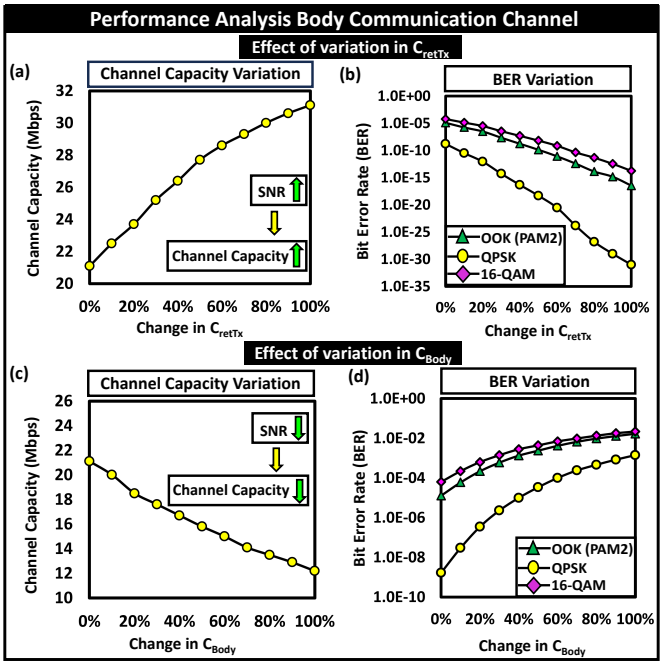

Fig. 6: Analyzing the effect of variation in C_{retTx} and C_{Body} on the performance metrics like channel capacity, Bit-error rate (BER) for EQS HBC: (a) Channel capacity variation with C_{retTx}, (b) BER variation with C_{retTx}, (c) Channel capacity variation with C_{Body}, (d) BER variation with C_{Body}

Additional Details of Experimental Setup

A. Calibration of Wearable Transmitter

With its ground being floating, the wearable Tx requires to be calibrated against a benchtop ground-connected standard. By connecting the transmitter to a benchtop oscilloscope while varying its frequency in the EQS regime from 100 kHz to 20 MHz, the peak-peak voltage shown in the oscilloscope is recorded, and the calibration correction for the Tx is calculated.

B. Calibration of Wearable Receiver:

The receiver is calibrated by connecting it to a Keysight signal generator, a benchtop standard. The output power of the benchtop signal generator varied over different power levels while varying the frequency from 100 kHz to 20 MHz, and the power difference observed between the two devices is noted to calculate the correction factor for the tinySA.

C. Calibration of Buffer:

The buffer's input connects to the output of a benchtop function generator, while the buffer's output is connected to a benchtop signal analyzer. The buffer's correction factor is then recorded.

D. Signal coupler at Tx & Rx

The signal coupler at Tx and Rx side is made of a commercially available double-sided conductive copper foil tape,

measuring 3.5 cm $\times$ 4.5 cm, and of $<$ 0.1 cm thickness, affixed to the bottom surface of the cut-board, ensures contact with the subject's skin.

E. System Schematic Diagram

The schematic of the measurement system shown in Fig. 7 illustrates the signal processing pipeline.

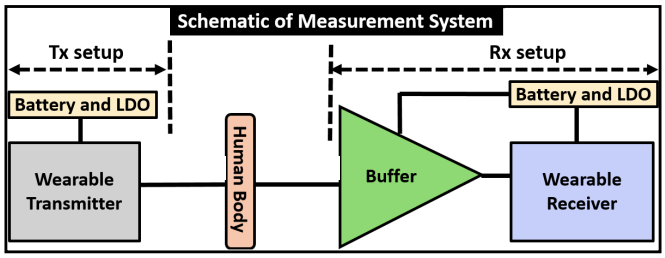

Fig. 7: The wearable transmitter (Tx) with its signal coupler in contact with the user's skin couples EQS signal to the body. A capacitive receiver (Rx) at the wrist of another arm is used to measure received voltage. The receiver setup includes the Tiny SA spectrum analyzer together with Buffer, c. Customized Buffer with high impedance capacitive termination for voltage mode communication

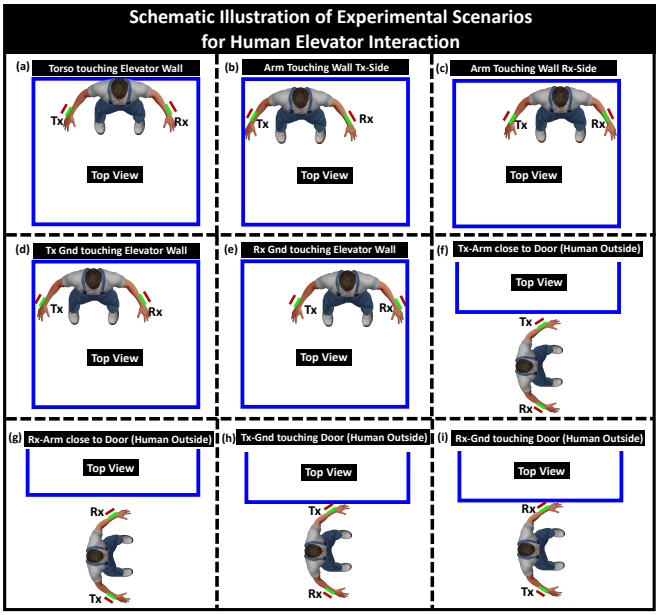

Fig. 8: Experimental Scenarios of interaction between EQS HBC user & Elevator: (a) Torso touching elevator wall, (b) Arm touching wall Tx-Side, (c) Arm touching wall Rx-Side, (d) Ground of Tx touching elevator wall, (e) Ground of Rx touching elevator wall, (f) Arm with Tx close to Door (Human Outside), (g) Arm with Rx close to Door (Human Outside), (h) Ground of Tx touching Door (Human Outside), (i) Ground of Rx touching Door (Human Outside)

VII. Schematic Illustration of the Experimental Scenarios

This section provides a schematic representation of the experimental scenarios involving the interaction between an EQS HBC subject and the elevator walls, as illustrated in Supplementary Fig. 8. The proximity to the elevator walls affects the parasitic return path capacitances, resulting in variations in transmission loss. The scenarios depicted in Supplementary Figs. 8 (a, b, c) shows changes in the locations of touch-based interactions between the subject and the elevator walls. In contrast, Supplementary Figs. 8 (d, e) presents scenarios where the ground of the transmit (Tx) and receive (Rx) components comes into contact with the elevator walls. Supplementary Figs. 8 (f, g) illustrates proximity-based interactions when the individual is outside. Finally, Supplementary Figs. 8 (h, i) depicts scenarios where the ground of the Tx and Rx components makes contact with the elevator door while the person is outside. This section presents a diagrammatic representation of the experimental setup involving the interaction between an EQS HBC subject and a vehicle, as illustrated in Supplementary Fig. 9. The subject's distance from the car door affects the parasitic return path capacitances, resulting in changes in transmission loss. The scenario depicted in Supplementary Fig. 9 (a) illustrates the subject seated in the middle seat of the car. In contrast, Supplementary Figs. 9 (b, c) showcase situations where the ground connections of the transmit (Tx) and receive (Rx) components make contact with the car door. Supplementary Figs. 9 (d, e) demonstrates the situation when the subject reaches their arm out of the car window. Lastly, Supplementary Fig. 9 (f) portrays scenarios in which the subject stands outside the vehicle.

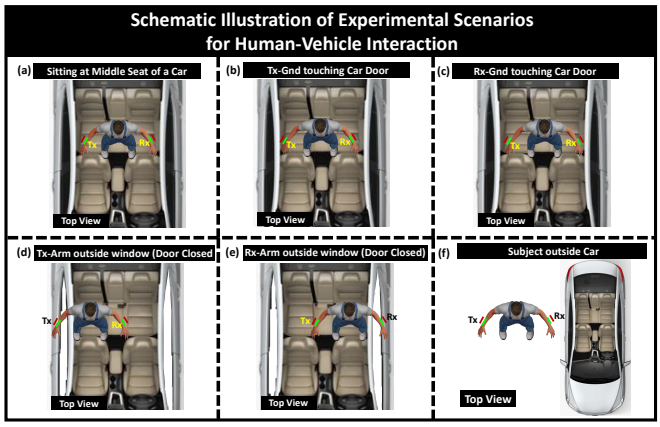

Fig. 9: Experimental Scenarios of interaction between EQS HBC user & Car: (a) Subject seating at middle seat of the car, (b) Ground of the Tx touching car door, (c) Ground of Rx touching car door, (d) Arm with Tx outside car window (Door Closed), (e) Arm with Rx outside car window (Door Closed), (f) Subject outside car